A study of hoof biomechanics using a finite element model

Glenn Ramsey, Peter Hunter, Martyn Nash

Auckland Bioengineering Institute, The University of Auckland, New Zealand

1 Introduction

Many aspects of hoof biomechanics are poorly understood. Experimental studies have increased our understanding of the hoof by measuring different aspects of its mechanical function. However there are many aspects that cannot be measured. Modelling is a process in which we attempt to recreate aspects of a physical system in order to study it in a controlled environment or to make predictions about the behaviour of that system in the real world. Modelling is an appropriate way to gain insight into hoof biomechanics where measurements are not possible.

In this work a finite element model of the hoof was used. The model allowed for varations in geometry, tissue properties and loading conditions. Results from 4 different modelling studies are presented. These studies investigate: the effects of varying hoof capsule properties due to moisture content; the effect of loading conditions on hoof mechanism; the effect of palmar angle on dorsal lamellar load; and the effect of solar surface shape on load distribution in the hoof capsule.

2 The influence of tissue hydration on equine hoof capsule mechanics

The mechanical properties of equine hoof horn are known to vary greatly with changing moisture content and this property is sometimes utilised for interventions that attempt to reshape the hoof capsule. However, the relationship of moisture content modulation to the mechanics of the whole hoof is unknown. This study explores the effect of moisture variation on hoof capsule mechanics and, in particular, deflections and elastic energy variations in the hoof.

A finite element model of the hoof was used. The hoof capsule tissue was modelled using finite elasticity with a heterogeneous transversely isotropic material relation, in which the elastic parameters were varied according to the moisture content of the tissue. The laminar junction and sole corium were modelled using an exponential Fung-type constitutive relation fitted to published data. The distal phalanx bone was modelled as a homogeneous isotropic material. Substrate interaction was modelled by contact with a rigid plate and loads typical of a trot were applied. Different scenarios were modelled where the moisture content of the hoof wall was varied from 40% to 100% of the fully hydrated case.

Results demonstrated that hoof capsule deflections and elastic energy in the capsule increased monotonically with increasing moisture content. Elastic energy in the laminar junction and sole corium remained constant. Hoof capsule deflections were within the experimentally reported range. A diagram of the model and the deflection results are shown in figure 1.

The mechanical behaviour of the hoof capsule is sensitive to variation in its moisture content. Experimental validations of hoof models should control for moisture content to improve reliability. Hoof capsule deflections may be amplified by increasing tissue hydration, and vice-versa. These results support hoofcare practices that involve manipulating the moisture content of the hoof.

3 The effect of loading conditions on hoof mechanism

A heel first landing is considered to be an indicator of a properly functioning hoof. It is thought that it encourages the development of a thick frog and digital cushion, which assist in the ability of the hoof to dissipate ground impact forces. A heel first landing is associated with a caudal point of force location but the effects of point of force location on the capsule have not been studied. A wide range of experimental measurements of heel expansion and other hoof deflections have been reported in the literature. One reason for these differences may be variations in hoof geometry but the effect of loading conditions and contact friction may also contribute.

The objective of this study was to determine the effect of changes in loading and contact friction on hoof deflections and elastic energy storage.

A range of boundary conditions were applied to finite element models. For all cases a load of 10 N/kg body–weight typical of the peak load in the trot gait, was used. In one scenario, a joint moment of 0.25 Nm/kg body–weight was used, and contact friction varying from frictionless to a frictional coefficient of 1.0 was used to simulate the effects of differing ground surfaces. In the other scenario a joint moment varying from 0 to 0.5 Nm/kg body–weight was used to move the centre of force cranially, simulating unloading of the heels. For all cases deflections and stored elastic energy for the different tissues were calculated.

Both increasing the contact frictional coefficient and moving the centre of force cranially caused the hoof capsule deflections and stored elastic energy to decrease. Peak strain energy in the capsule occurred when the frictional coefficient was 0 and when the joint moment was 0, for the friction and centre of force scenarios, respectively. Minimum strain energy occurred when the frictional coefficient was 1.0 and when the joint moment was 0.4 Nm/kg body–weight.

Hoof expansion and elastic energy storage are considerably influenced by ground surface friction and point of force location. As *in vivo* loading conditions can be variable, model validation studies should account for these differences. The amount of hoof expansion is correlated with the capacity of the hoof to store elastic energy. These results indicate that maximising the energy absorption may be the purpose of heel first landing.

4 The effect of hoof angle variations on dorsal lamellar load in the equine hoof

In the treatment of laminitis, it is believed that reducing tension in the deep digital flexor tendon by raising the palmar angle of the hoof can reduce the load on the dorsal lamellae, allowing them to heal or to prevent further damage. The objective of this study was to determine the effect of alterations in hoof angle on the load in the dorsal laminar junction.

Biomechanical finite element models of equine hooves were created with palmar angles of the distal phalanx varying from 0° to 15°. Tissue material relations accounting for anisotropy and the effect of moisture were used. Loading conditions simulating the stages in the stance where the vertical ground reaction force, the mid–stance joint moment, and the breakover joint moment were maximal, were applied to the models. The loads were adjusted to account for the reduction in joint moment caused by increasing the palmar angle. Models were compared using the stored elastic energy, an indication of load, which was sampled in the dorsal laminar junction.

For all loading cases, increasing the palmar angle increased the stored elastic energy in the dorsal laminar junction. The stored elastic energy near the proximal laminar junction border for a palmar angle of 15° was between 1.3 and 3.8 times that for a palmar angle of 0°. Stored elastic energy at the distal laminar junction border was small in all cases. For the breakover case, stored elastic energy at the proximal border also increased with increasing palmar angle. Figure 2 shows some of these results.

The models in this study predict that raising the palmar angle increases the load on the dorsal laminar junction. Therefore hoof care interventions that raise the palmar angle in order to reduce the dorsal lamellae load may not achieve this outcome.

5 The effect of ground bearing surface shape on load distribution in the equine hoof capsule

A large number of horses have contracted heels, which can lead to lameness and therefore an incapacitated horse. Heel contraction is quantified by a low width to length ratio of the foot's frog (homologous to the foot pad in other ungulates). It is known that lack of load on the hoof (such as when it is injured), a long–toe–low–heel conformation, or the prolonged use of iron horseshoes can cause contraction, however the underlying mechanism is not understood. If the cause of contraction could be elucidated then measures could be taken to prevent it. This study investigated the effects of common hoof shape variations on the distribution of ground surface contact pressure and on the distribution of strain in the hoof wall.

Finite element models were created to represent (i) flat weight–bearing on a normal hoof; (ii) a hoof with under–run heels (where the heel is more sloped than the toe); (iii) a hoof with weight–bearing bars (the bar is an inward turned continuation of the hoof wall); (iv) a hoof with an iron horseshoe; (v) a hoof with concave lateral wall relief (as observed in naturally worn hooves). The models were configured as frictionless contact mechanics problems using a rigid substrate. Boundary conditions simulating the maximal load in a trot gait were applied.

The models with a flat weight–bearing surface, substrate contact on the bar, and a horseshoe each showed that contact pressure was distributed away from the heels and was maximal in the contact region cranial to the caudal edge of the distal phalanx. These models, plus the case of under–run heels, indicated a region of low strain in the wall proximal to the heel. In models with a 1mm concave wall relief, the contact pressure was concentrated at the toe and heel contact points at the onset of loading. However, at the maximal load it was distributed more evenly along the bearing surface of the wall, since the relief was flattened out during loading. These models did not have a region of low strain in the wall at the heel. Figure 3 shows some of these results.

Based on these results, we propose that a level ground bearing surface of the hoof causes redistribution of load away from the heels, which in turn allows the heels to become contracted. On the other hand, this is not expected in healthy naturally worn hooves, because the concave shape of the bearing surface causes the heels to carry load. The predicted strain distributions suggest that the caudal part of the hoof is cantilevered by the distal phalanx. This explains the contact pressure distributions, which are consistent with the concave bearing surfaces that have been observed in naturally worn hooves. Understanding the cause for contraction and for the shape of the naturally worn hoof may lead to improvements in hoofcare practices.

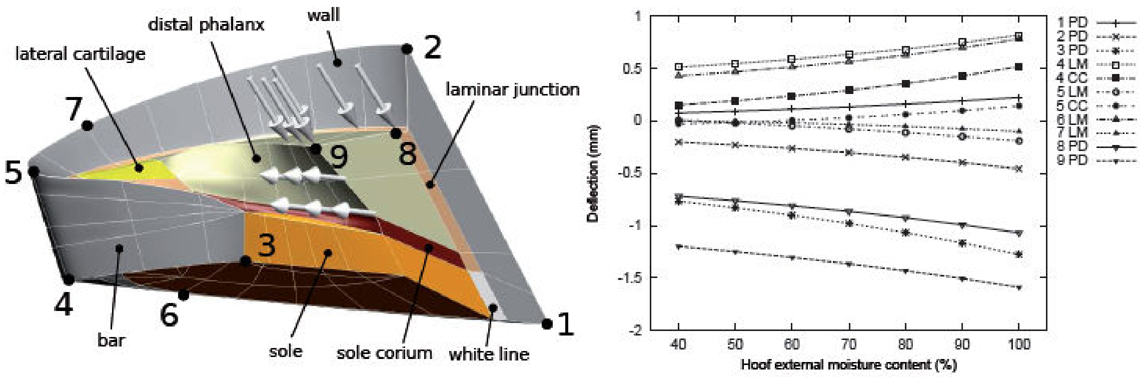

Figure 1: Rendering of hoof model (left) and deflections (right) for external hoof moisture content varying from 40% to 100% of the fully saturated amount. Numerical labels correspond to locations on the left figure. Alphabetical labels indicate deflection direction: proximo–distal (PD), latero–medial (LM), cranio–caudal (CC).

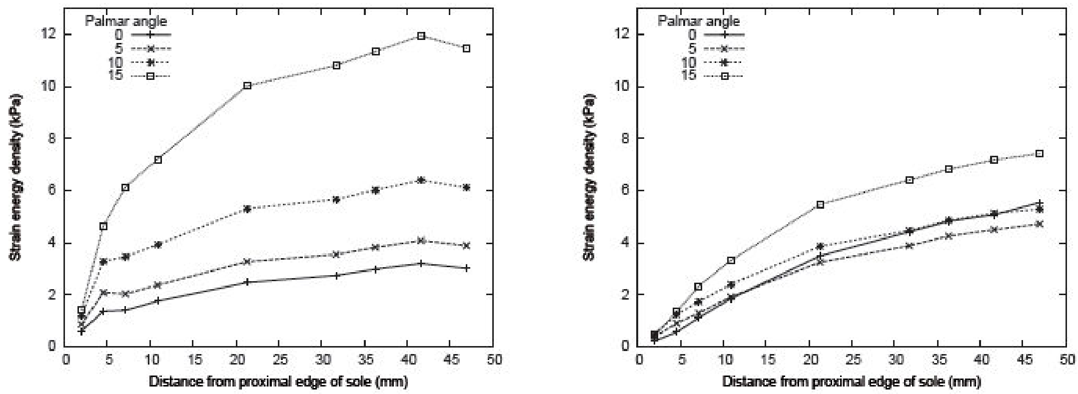

Figure 2: Strain energy density in the dorsal laminar junction, at the walk, for palmar angles varying from 0° to 15°, for the peak vertical ground reaction force (left) and breakover (right) stages of the stance.

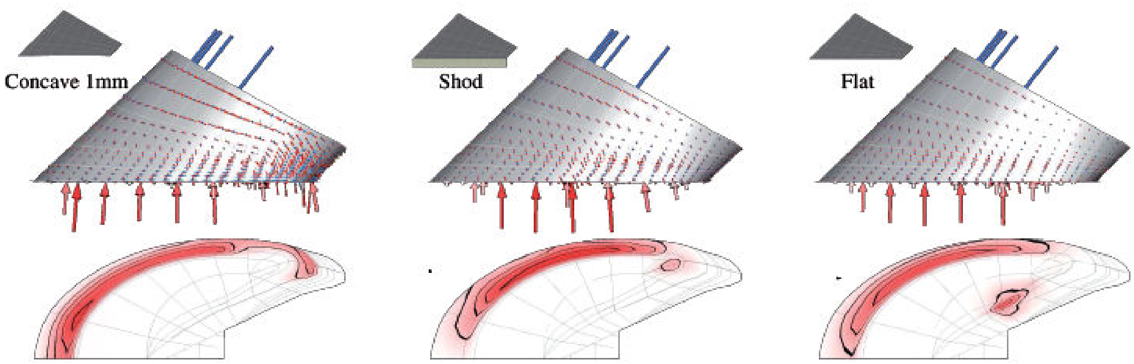

Figure 3: Effect of 1mm concave (left), horseshoe (centre) and flat (right) ground contact surface shapes on contact pressure distribution on the solar surface of the hoof wall and strain distribution in the wall.